MOUNTAIN-PLAINS CONSORTIUM

MPC 22-483 | J. Tanner and S.P. Buenfil

EVALUATION OF CONCRETE BRIDGE DECK MIXTURES USING SHRINKAGE-RING TESTS

A University Transportation Center sponsored by the U.S. Department of Transportation serving the Mountain-Plains Region. Consortium members:

Colorado State University
North Dakota State University
South Dakota State University
University of Colorado Denver
University of Denver
University of Utah
Utah State University
University of Wyoming

Technical Report Documentation Page

1. Report No.	2. Government Accession No.	3. Recipient's Catalog No.
MPC-652		

4. Title and Subtitle Evaluation of Concrete Bridge Deck Mixtures Using Shrinkage-Ring Tests	5. Report Date December 2023 6. Performing Organization Code
7. Author(s) Jennifer Tanner Shamel Perez Buenfil	8. Performing Organization Report No. MPC 22-483
9. Performing Organization Name and Address Dept. of Civil & Architectural Engineering and Construction Management Department of Mathematics & Statistics University of Wyoming 1000 E. University Ave. Laramie, WY 82071	10. Work Unit No. (TRAIS) 11. Contract or Grant No.
12. Sponsoring Agency Name and Address Mountain-Plains Consortium North Dakota State University PO Box 6050, Fargo, ND 58108	13. Type of Report and Period Covered Final Report 14. Sponsoring Agency Code

15. Supplementary Notes

Supported by a grant from the US DOT, University Transportation Centers Program

16. Abstract

The aim of this document is to evaluate and compare concrete mixture designs using a granitic aggregate and employing mitigation measures. Specific measures include polypropylene fibers and shrinkage reducing admixture (SRA). Four different mixture designs were evaluated: control, addition of 8 lb/yd3 (4.75 kg/m3) of polypropylene fibers, dosage of 2% SRA by weight of cementitious material, and the combination of both mitigation methods.

Two experimental approaches were carried out to assess restrained shrinkage: single-ring and dual-ring. Mechanical properties such as compressive and tensile strength were studied for each mixture. Results indicated that incorporating fibers into the mixture roughly doubles the time to cracking. Adding SRA into the mix increased the cracking age by 90%. The combination of 8 lb/yd3 (4.75 kg/m3) of fibers with 2% of SRA replacement proved to be the most effective measure for extending cracking time—improving it by an average of five times the original cracking.

17. Key Word	18. Distribution Statement
bridge decks, concrete bridges, cracking, ring stress, shrinkage, test procedures	Public distribution

19. Security Classif. (of this report)	20. Security Classif. (of this page)	21. No. of Pages	22. Price
Unclassified	Unclassified	43	n/a

Form DOT F 1700.7 (8-72) Reproduction of completed page authorized

Evaluation of Concrete Bridge Deck Mixtures Using Shrinkage-Ring Tests

Jennifer Tanner
Shamel Perez Buenfil

University of Wyoming
Laramie, Wyoming

December 2023

Acknowledgements

This work was supported by the Mountain-Plains Consortium. The authors are grateful for their investment.

Disclaimer

ABSTRACT

The aim of this document is to evaluate and compare concrete mixture designs using a granitic aggregate and employing mitigation measures. Specific measures include polypropylene fibers and shrinkage reducing admixture (SRA). Four different mixture designs were evaluated: control, addition of 8 lb/yd^3 (4.75 kg/m^3) of polypropylene fibers, dosage of 2% SRA by weight of cementitious material, and the combination of both mitigation methods.

Two experimental approaches were carried out to assess restrained shrinkage: single-ring and dual-ring. Mechanical properties such as compressive and tensile strength were studied for each mixture. Results indicated that incorporating fibers into the mixture roughly doubles the time to cracking. Adding SRA into the mix increased the cracking age by 90%. The combination of 8 lb/yd^3 (4.75 kg/m^3) of fibers with 2% of SRA replacement proved to be the most effective measure for extending cracking time—improving it by an average of five times the original cracking.

TABLE OF CONTENTS

LIST OF FIGURES

LIST OF TABLES

1. INTRODUCTION

1.1 Background

Concrete is widely utilized due to its versatility, strength, durability, and affordability. It is a composite material comprised of cement, water, coarse aggregates, fine aggregates, and admixtures, which are combined to achieve desired properties. Although concrete has been widely studied, there are some uncertainties about its behavior during the curing process, where restrained concrete undergoes volume changes that can result in early-age cracking. In the context of bridges, cracks can lead to corrosion and decrease the deck's lifespan. Currently, the cost of maintenance of concrete on bridge decks represents a significant part of Wyoming DOT's budget. It is essential to further understand the reasons why shrinkage happens and, subsequently, to evaluate best practices to mitigate concrete shrinkage.

Shrinkage can be categorized as autogenous, plastic, drying, carbonation, and thermal (Elzokra, et al. 2020). The total shrinkage of concrete can be divided into two types: (a) early-age shrinkage, which occurs within the first 24 hours after mixing, and (b) long-term shrinkage, which encompasses the subsequent period (Lofgren and Esping 2006). Early-age shrinkage can be attributed to drying, thermal, or autogenous shrinkage; long-term shrinkage is associated with those three types plus carbonation shrinkage (Holt 2001). Long-term shrinkage occurs because of loss of water from the hydrated cement paste, internal reactions, or temperature changes.

There are various methods to mitigate shrinkage. One is the use of shrinkage reducing admixtures (SRAs) that are designed to reduce drying shrinkage and, as a result, long-term cracking. Their use has been increasing over the past few years and therefore it is essential to evaluate their impact on other mechanical properties. Another remedy to reduce shrinkage is adding fibers to the concrete mix that act as a reinforcement to enhance concrete tensile strength.

Despite the well-established knowledge of shrinkage's impact on durability, there are limited validated methods available for mitigating this issue. As a result, it is crucial to assess the effectiveness of different approaches in reducing shrinkage by evaluating the performance of various concrete mixes.

1.2 Research Objectives

The primary objective of this study is to evaluate and compare concrete mixture designs using mitigation methods using polypropylene fibers and shrinkage reducing admixture. The evaluation specifically focuses on granite aggregates using the single- and dual-ring tests to assess shrinkage.

2. LITERATURE REVIEW

2.1 Types of Shrinkage

Ultimate strength design is important; nevertheless, the serviceability of the structure is also significant. Part of the serviceability requirements involve controlling cracking. When shrinkage is present on a restrained structure, such as concrete deck bridges, stresses develop. If these stresses surpass the tensile strength of concrete, cracking occurs (Zhan and He 2019). Concrete shrinkage can be classified into several types: autogenous, plastic, drying, carbonation, and thermal shrinkage; each has its own characteristics and causes.

Autogenous, drying, and thermal shrinkage can occur at both early and later stages, causing overlap between them and adding their effects into cracking (Linmei, et al. 2017). The bulk of shrinkage is due to autogenous and drying shrinkage, as shown in Figure 2.1, and it will be discussed in the following section, Autogenous Shrinkage.

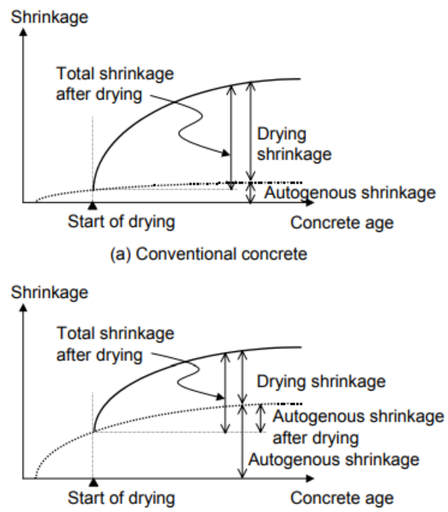

Figure 2.1 Shrinkage in conventional and high-strength concrete (Sakata and Shimomura 2004)

2.1.1 Autogenous Shrinkage

Autogenous shrinkage of cement pastes results in volume change caused by chemical reactions during hydration. Temperature variation and water loss are not part of this kind of shrinkage. Autogenous shrinkage is determined by several variables such as cement chemical composition, fineness of cement, water/cement ratio, reaction temperature, and presence of admixtures (Van breugel 1998). It is necessary to study how these parameters can reduce volume changes associated with this type of shrinkage to avoid micro-cracking during the hardening process.

Autogenous shrinkage is smaller than the total shrinkage. It has been shown that autogenous shrinkage of low water-cement ratio concrete can reach the same values as drying shrinkage while the difference increases as the water-cement ratio increases as well (Tazawa and Miyazawa 1995). A 2018 study showed that for regular-strength concretes of 30 MPa, autogenous shrinkage is approximately 25% of the total shrinkage. On the other hand, high-strength concrete showed that roughly 50% of the total strain was due to autogenous shrinkage by comparing the right sides of Figure 2.2 a and b (Gilbert, et al. 2018).

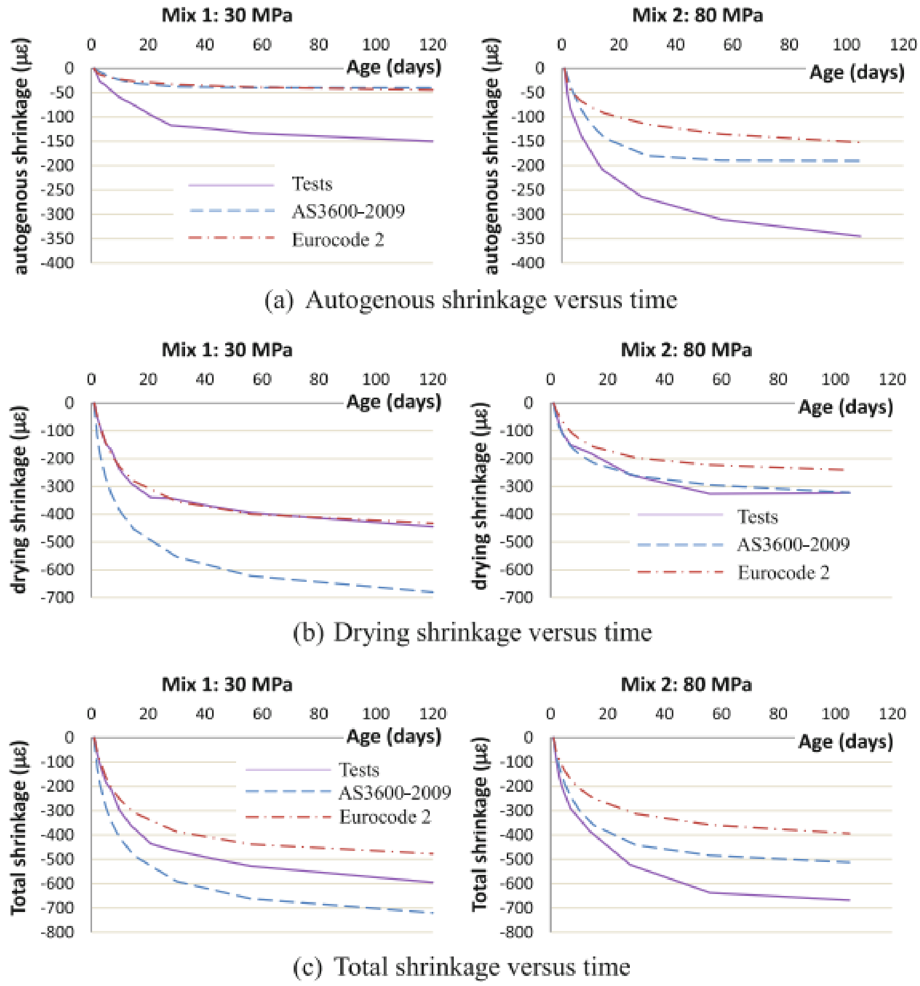

(a) Autogenous shrinkage versus time

(b) Drying shrinkage versus time

(c) Total shrinkage versus time

Figure 2.2 Shrinkage strains comparisons (Gilbert, et al. 2018)

As shown in Figure 2.3, autogenous shrinkage decreases when the water/cement ratio is increased, and most of this shrinkage occurs within the first 24 hours (Holt 2005).

The most effective method to reduce autogenous shrinkage has proven to be moist curing. However, it is imperative to emphasize that shrinkage may still occur even when concrete is subjected to 100% moist curing (Holt 2005).

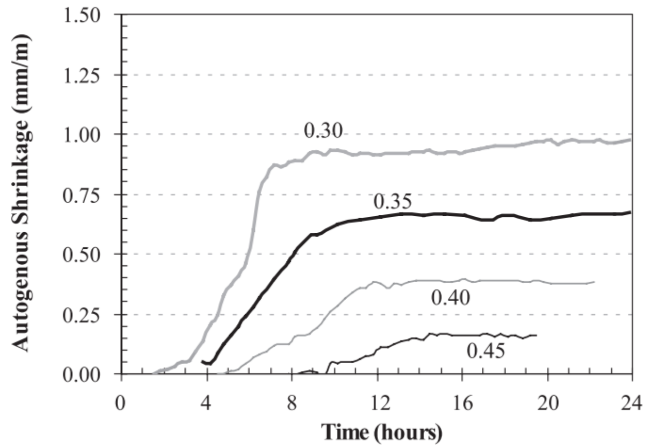

Figure 2.3 Autogenous shrinkage resulting with changing w/c ratio and equivalent water amount (Holt 2005)

Currently, there is no standardized procedure to measure autogenous shrinkage. For this reason, many researchers use different measurement techniques that are adapted to the requirements for their experiments (Tang, Huang and He 2021) (Gilbert, et al. 2018).

2.1.2 Plastic Shrinkage

Plastic shrinkage occurs when fresh concrete loses moisture to reach equilibrium with the environment right after casting and before hardening. This type of shrinkage occurs when the concrete is fresh during the plastic state. Both types of variables that affect this type of shrinkage are concrete composition and environmental conditions like ambient temperature, humidity, and content of cementitious materials (Elzokra, et al. 2020).

When the environmental conditions are dry, plastic shrinkage is more likely to develop due to rapid moisture loss and low rate of bleeding during the setting. Plastic shrinkage cracks are usually small but may extend to several feet and can represent a problem on the structure because they can allow the infiltration of external agents into the concrete.

In addition to moisture loss, three more primary factors can induce plastic shrinkage. For reinforced concrete, differential settlement of a restrained section can induce stresses. Another factor is thermal differential movement that will be discussed in Thermal Shrinkage. The third factor is autogenous shrinkage. These factors either can act together or independently to increase the probability of cracking (Weiss 2022).

In 2013, an investigation showed that the addition of synthetic fibers at low volumes effectively reduce the plastic shrinkage cracks (Boshoff and Combrinck 2013). Coarse fibers are less efficient than finer fibers while reinforcing concrete (Qi, Weiss and Olek 2003). ASTM C1579 proposes a methodology of how to evaluate plastic shrinkage of restrained fiber reinforced concrete. The purpose of this test is to evaluate the effects of evaporation, settlement, and early autogenous shrinkage on the plastic shrinkage cracking performance before setting (ASTM C1579 2021). Mix composition significantly affects plastic shrinkage. Increasing water-cement ratio increases both bleeding and rate of evaporation (Almusallam, et al. 1998).

By understanding plastic shrinkage behavior, it is possible to mitigate the risk of plastic shrinkage cracks. Studies have shown several ways of preventing them, such as reducing the concrete temperature, fog sprays, or placing concrete in the morning (White 1975).

2.1.3 Drying Shrinkage

Drying shrinkage is the continuation of moisture evaporation as concrete hardens and gains strength. This type of shrinkage results in three different mechanisms: capillary stress, disjoining pressure, and surface free energy. The evolution of drying shrinkage is a process that takes more time compared with other types of shrinkage like autogenous or plastic shrinkage. Several factors influence drying shrinkage, such as concrete proportions, construction practices, and environmental conditions (Hasan 2020). Bridge decks are more susceptible to cracking induced by drying shrinkage because they have a larger surface area to volume ratio (Gribniak, Kaklauskas and Bacinskas 2007).

Coarse aggregates in concrete physically restrain the shrinkage of hydrating and drying cement paste, depending on the ratio between the modulus of elasticity of the aggregate and paste. Larger aggregates can prevent microcracks due to shrinkage from developing into macro cracks (Karagüler and Yatağan 2018). Historically, studies have shown that using different kinds of aggregates can have an impact on drying shrinkage in th e range of 120% to 150% (Powers 1959), (Meininger 1966), and (Tremper and Spellman 1963).

The type and duration of curing can affect the rate and ultimate amount of drying shrinkage. Curing compounds, sealers, and coatings can trap free moisture in the concrete for long periods, resulting in delayed shrinkage. Wet curing methods, such as fogging or wet burlap, hold off shrinkage until curing is terminated, after which the concrete dries and shrinks at a normal rate (Kosmatka and Wilson 2011). Another study showed that when using admixture surface treatments, such as silane-treated carbon fibers, the effects of cement paste's drying shrinkage were reduced by 32% (Xu and Chung 2000). In 2019, a study was conducted to evaluate the alkali activated binders on drying shrinkage compared with normal Portland cement (Matalkah, et al. 2019). The results showed that drying shrinkage on alkali activated binders concrete was about twice that of Type I Portland cement and that the use of some additives can reduce the shrinkage but also reduce the mechanical strength of concrete.

2.1.4 Carbonation Shrinkage

Carbonation shrinkage is a chemical reaction leading the concrete to reorganize its microstructure and decrease its porosity. In this process, concrete absorbs CO_2 in the atmosphere. Carbonation shrinkage is restrained by sand particles, which makes concrete less prone to cracking than mortar (Houst 1997).

2.1.5 Thermal Shrinkage

Thermal shrinkage results from a decrease in concrete temperature due to the difference between it and the ambient conditions and typically occurs in the first 12 hours (Holt 2005). There is evidence that time of pouring has relevance on the concrete's strength development, with a higher early strength for concretes poured at higher temperatures that, consequently, may induce early cracking (Sofi, et al. 2014).

The effect of the type of aggregate on early-age thermal cracking of concrete has been studied (Chilwesa, et al. 2020). This study concluded that the aggregate influences the cracking potential of concrete, where mixes made with basalt and limestone performed better compared with those made with granite. This study also reported that the use of the dual-ring test to assess shrinkage and expansion subjected to various temperatures is very similar to field conditions.

2.2 Assessment of Early-age Cracking

A study conducted by Xi et al. (2003) focused on the assessment of cracking in newly constructed bridge decks in Colorado to identify the causes and extent of cracking in these structures. Their findings highlighted various factors that contributed to cracking, including shrinkage, temperature variations, concrete mix design, construction practices, and environmental conditions. The study emphasized the importance of considering these factors during the design and construction phases to minimize cracks and proposed recommendations for mitigation measures (Xi, et al. 2003).

In 2018, Bolander developed a model that simulates the early-age behavior of structural concrete, focusing on cracking of concrete bridge decks and slabs (Bolander 2018). The article emphasizes the importance of proper joint spacing, reinforcement detailing, and curing techniques to control cracking.

It is possible to study the effects of variables like hydration effects, curing methods, mix design, and addition of admixtures by measuring strain in a steel ring that restrains a concrete ring. A full description is available in Section 4.

The dual-ring test is a relatively new method to assess cracking in concrete specimens, but there has been a notable increase in the utilization of this test because of its advantages. These studies demonstrated that the dual-ring is a good method to characterize cracking propensity of different types of concrete (De la Varga, Spragg and El-Helou, et al. 2019), (Wilson and Weiss 2020), and (De la Varga, Spragg and Muñoz, et al. 2018). This test is modified to provide the same degree of restraint of the ASTM C1581 (Schlitter, et al. 2010).

2.3 Mitigation Methods

Mitigation methods are intended to effectively address these concerns and enhance the performance and longevity of concrete. Common mitigation approaches utilize shrinkage-reducing admixtures, internal curing, incorporating fibers or reinforcement, employing proper curing techniques, ensuring well-designed joints and their accurate placement, as well as controlling environmental conditions during construction. These methods collectively contribute to reducing shrinkage, controlling cracking, and bolstering the overall quality and durability of concrete structures. It is crucial to focus on early shrinkage mitigation since concrete exhibits its lowest strength capacity during that period, thus minimizing the risk of early-age cracking.

2.3.1 Fibers

In restrained structures, shrinkage leads to the development of cracks in concrete that vary in size and shape depending on the specimen conditions such as size, aspect ratio, supports, temperature, relative humidity, designed strength, and others. A widely used procedure to prevent cracks in concrete caused by shrinkage is to add fibers to concrete. In general, fibers sew around cracks by creating a bond between the aggregates. This allows concrete to behave as a ductile material instead of a brittle material. Adding fibers to the concrete mixture can reduce plastic shrinkage cracking up to 80% (Pillar and Repette 2015). Polypropylene fibers have a positive impact on early-age shrinkage but can reduce slump (Myers, Kang y Ramseyer 2008).

The combination of fibers with other mitigation methods such as expansive agents (5%-10%), SRA (1%-2%), and saturated lightweight sand (10%-25%) has been studied. The ternary combination of those three mitigations methods with fiber reinforced concrete demonstrated a decrease in the total shrinkage. The addition of these mitigation methods may reduce both compressive and flexural properties (Aghaee and Khayat 2021).

A 2005 study was developed that focused on the restrained shrinkage behavior of mixtures that incorporate both shrinkage-reducing admixtures and fibers. The study aimed to understand how these additives interact and influence the shrinkage properties of concrete. They concluded that the addition of fibers effectively increases the amount of energy that can go into crack development before the cracks become visible, while the addition of SRA decreases the microcracking (Pease, Weiss and Shah 2005).

2.3.2 Admixtures

Chemical admixtures are added to the mixture to enhance concrete properties. Shrinkage reducing admixtures (SRAs) have a positive impact on the durability of concrete by mitigating shrinkage by delaying the hydration process; but this also leads to a delay in the hardening, which can reduce the compressive strength at early ages (Maia, et al. 2012).

SRA molecules work by reducing the polarity of the paste solution, which leads to the hydration retardation of tricalcium silicate and reducing the peak temperature (Zhan y He 2019). SRAs have shown major changes in the hydration dynamics: a later hydration that leads to a decrease in the maximum temperature of the reaction (Maia, et al. 2012).

Several studies have shown that the addition of SRAs to the concrete mix decreased the compressive strength of the concrete up to 20%, more remarkably at early ages (Maia, et al. 2012), (Güneyisi, Gesoglu, et al. 2014), (Yoo, et al. 2015), and (Oliveira, Ribeiro and Branco 2014). However, other studies that have shown an improvement in the compressive strength of concrete (Wang, Banthia and Zhang 2012) and (Wang, Chia, et al. 2013).

It has been shown that the addition of SRAs effectively reduces the size of shrinkage cracks (Lura, y otros 2007). In 1992, Shh studied the efficiency of shrinkage-reducing admixtures to control restrained shrinkage cracking of concrete. The result of their work shows that SRAs significantly reduce free shrinkage, and there is a considerable reduction in crack width (Shh, Krguller and Sarigaphuti 1992).

2.4 Literature Review Conclusions

From the literature review, shrinkage consists in two major components: drying shrinkage and autogenous shrinkage (Gribniak, Kaklauskas and Bacinskas 2007). Early age shrinkage is most likely attributed to autogenous and thermal shrinkage, depending on the water/cement ratio of the concrete. Autogenous shrinkage decreases by increasing the water/cement ratio. Drying shrinkage is the most significant part of the total shrinkage. The use of fibers, shrinkage reducing admixtures, internal curing materials, and larger aggregates are an effective way to mitigate shrinkage.

3. MATERIALS

3.1 Cement

Type I/II Portland cement meeting ASTM C150 (2021) was used. The material used over the lifespan of the entire project was taken from a single batch to ensure that variations in concrete batches would not affect mixtures that were poured at different times.

3.2 Aggregates

The first set of specimens was made with granite aggregate supplied by WYDOT and is labeled GR. Mechanical properties were determined in accordance with ASTM C127 and ASTM C128.

3.2.1 Coarse Aggregates

Aggregates were sieved and modified to meet size 67 from ASTM C33. Granite properties are shown in Table 3.1.

Table 3.1 Coarse aggregate properties

	Granite
Dry Bulk Specific Gravity	2.53
Absorption	0.64%
Bulk Density	102.62 lb/ft^3 [1643.8 kg/m^3]

3.2.2 Fine Aggregates

The fine aggregate was modified to meet ASTM C33. Its properties are shown in Table 3.2.

Table 3.2 Fine aggregate properties

	Granite
Dry Bulk Specific Gravity	2.65
Absorption	1.63%
Bulk Density	114.73 lb/ft^3 [1837.8 kg/m^3]

3.3 Fibers

The fibers used (Figure 3.1) in this work were 1.5-inch blended copolymer macrofibers complying with ASTM C1116 (2015). The manufacturer's minimum content is three pounds per cubic yard. For the dual-ring mixtures, the maximum recommended fiber content, eight pounds per cubic yard (4.75 kg/m^3), was used.

Figure 3.1 Polypropylene fibers

3.4 Admixtures

Shrinkage reducing admixture (SRA) is an admixture specifically formulated to reduce drying shrinkage in concrete. In this work, EUCON SRA-XT was used to meet the requirements of ASTM C494/C494M. The maximum recommended dosage of 2% by weight of cementitious materials was used on this work.

3.5 Mixture Design

For this project, control mixtures were designed. A test matrix with the variables is shown in Table 3.3. In the naming convention, the first part is DR for dual-ring or SR for single ring, then GR for granite. The following part of the name starting with the letter F describes the pounds of fiber per cubic yard and the letter S designates the percent of water replaced by SRA. The final digit represents the number of days at which cooling began (Figure 3.2).

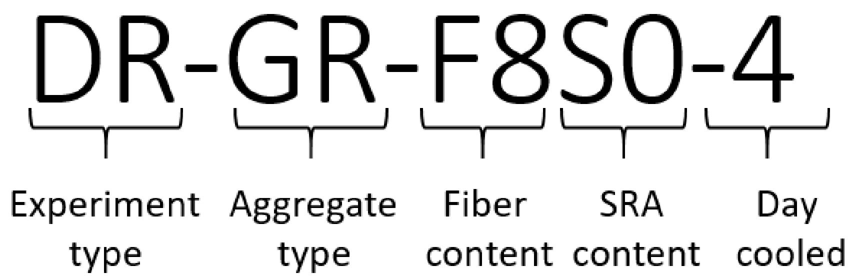

Figure 3.2 Naming convention

Table 3.3 Test matrix with variables for all experiments

Test Name	Mitigation Type
SR-GR-F0S0	Control
SR-GR-F8S0	8 lb/yd^3 (4.75 kg/m^3) fiber
SR-GR-F0S2	2% SRA
SR-GR-F8S2	8 lb/yd^3 (4.75 kg/m^3) fiber + 2% SRA
DR-GR-F0S0-4	Control
DR-GR-F8S0-4	8 lb/yd^3 (4.75 kg/m^3) fiber
DR-GR-F0S2-4	2% SRA
DR-GR-F8S2-4	8 lb/yd^3 (4.75 kg/m^3) fiber + 2% SRA

4. DESCRIPTION OF TEST METHODS

4.1 Single-ring Set Up

AASHTO T 334-08 and ASTM C1581 estimate the time to cracking of restrained concrete specimens (Figure 4.1). The procedure consists of a concrete sample in a circular mold around a steel ring instrumented with strain gages (Figure 4.2) (ASTM International 2018) and determines the effects of variations in the properties of restrained concrete measured as the time to cracking.

Figure 4.1 Single-ring test

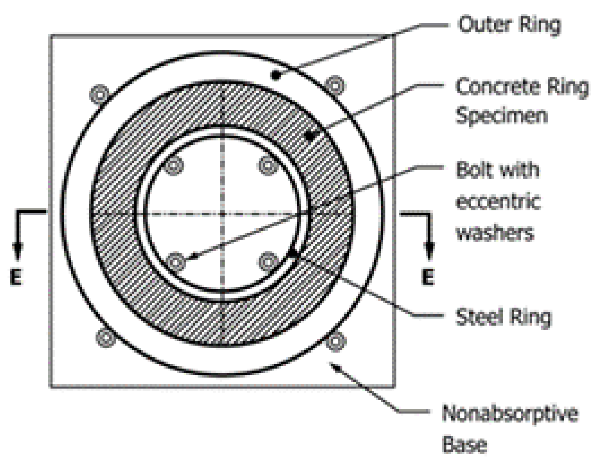

Figure 4.2 Plan view of the single-ring test

Several single-ring molds used were built to the dimensions specified in AASHTO T334, as shown in Figure 4.3. The molds consisted of a 20 x 20 in. (508 x 508 mm) plywood base with a plywood ring having an inner diameter of 18¼" (463.5 mm) attached to it to hold a six-inch strip of ⅛" (3.2 mm) thick high-density polyethylene (HDPE) to act as the outer mold. An identical plywood ring was placed on top of wooden spacer blocks at the top of the HDPE strip to provide rigidity during concrete placement, as seen in Figure 4.4. A six-inch-high (152 mm) steel ring with an inner diameter of 11” (280 mm) and an outer diameter of 12” (305 mm) was held to an inner circle of plywood by four wooden blocks equally spaced between the four strain gages on the interior of the ring. A polyethylene film was placed on the base plywood sheet to allow the specimen to move laterally.

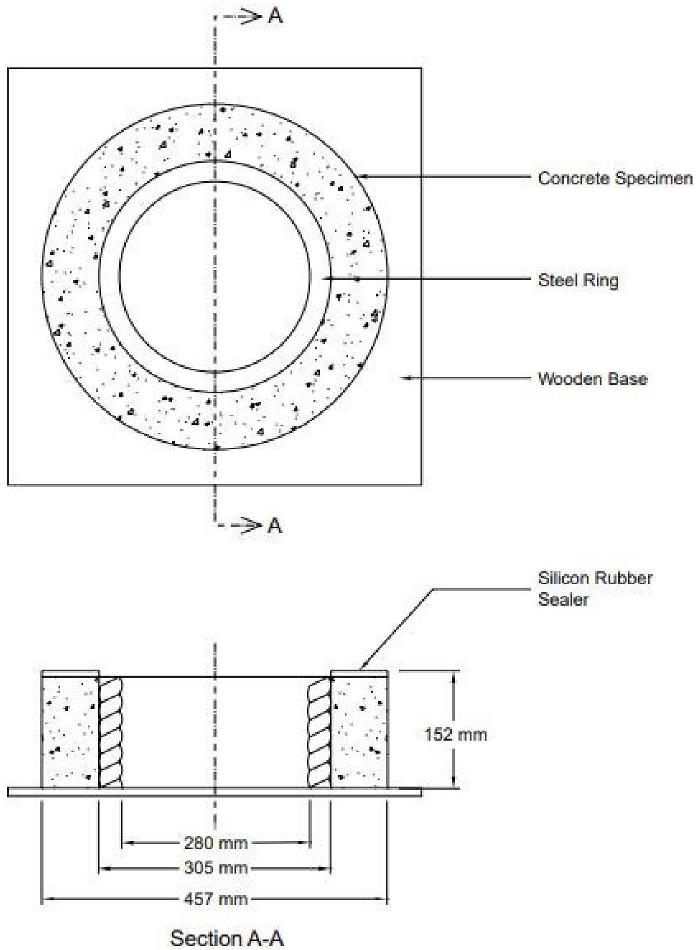

Figure 4.3 Single-ring specimen dimensions (not to scale, tolerance ±5mm) (AASHTO, 2022)

Figure 4.4 Single-ring test setup

4.1.1 Instrumentation

To record the strain data, four 5-mm strain gages were placed at quarter points around the inside of the steel rings at mid-height. Before the gages were attached, the rings were sanded to allow the strain gages to securely adhere. The strain gages were connected to a data acquisition system set to record data every five minutes for the first 24 hours, and every 30 minutes after five minutes.

4.1.2 Casting Procedures

The concrete was mixed in accordance with ASTM C305 and placed into the molds in three lifts and rodded 75 times for each lift. The concrete was finished with a hand trowel and a float. Approximately one hour after the specimens were poured, wet burlap was placed on top to promote curing. After 24 hours, the exterior HDPE molds were removed, and a plastic cover was affixed to the top of the rings using a silicone caulk to prevent moisture loss. The plywood base was lightly tapped with a mallet to break the rings free from the nonstick plastic on the base, but the specimens were left on their bases to prevent moisture loss through the bottom of the specimens. A single-ring specimen after the removal of the HDPE mold and plastic cover is shown in Figure 4.5. Note that some silicone caulk is still adhered to the specimen in the picture. Sample cylinders were broken at 28 days in accordance with (ASTM C39 2021) to determine the compressive strength.

Figure 4.5 Single-ring specimen after removal of plastic cover

4.2 Dual-ring Set Up

Dual-ring shrinkage tests evaluate the stress development and cracking potential due to restrained volume change. In this test, temperature and volume changes are controlled with strain gages placed at four equidistant quarter points on both the interior of the inner ring and the exterior of the outer ring (AASHTO 2017) along with thermocouples. This test uses two rings made of a low thermal expansion iron-nickel alloy (Invar) that remains stable under different temperature conditions (Figure 4.6).

Figure 4.6 Dual-ring test

Two testing apparatuses were built in accordance with AASHTO T363 to evaluate the early-age shrinkage behavior. To minimize the effects of temperature variation on the experiment, the rings were fabricated from low thermal-expansion iron-nickel alloy (Invar) with a thermal expansion coefficient of 1.3×10^{-6}/°C, as specified in ASTM F1684 (2021). The low coefficient of thermal expansion of the rings reduces the degree of restraint of the sample during a temperature change (Raoufi, et al. 2011). A lower coefficient of thermal expansion of Invar rings will allow temperatures to vary while the rings remain volumetrically stable. The dual-ring test setups were made following AASHTO T363. Dimensions of the rings are illustrated in Figure 4.7.

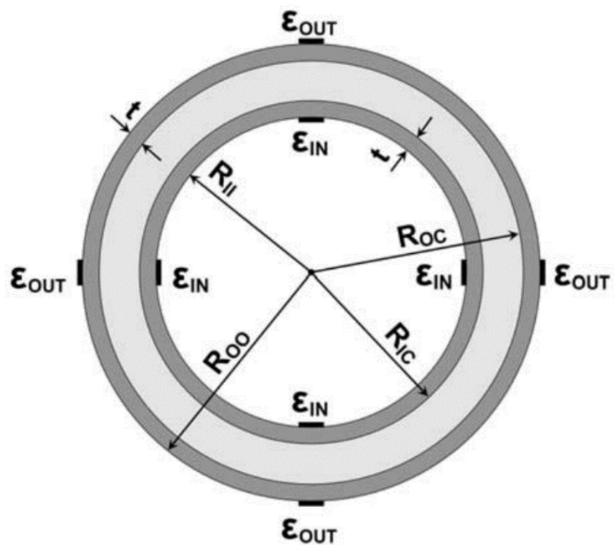

Ring Face	Radius (mm)
R_{II}	146 ± 3
R_{IC}	165 ± 3
R_{OC}	203 ± 3
R_{OO}	222 ± 3

Figure 4.7 Geometry of dual ring test. Source: (AASHTO, 2017)

4.2.1 Instrumentation

To determine the induced stress, the strain was measured in both the inner and outer rings. Each ring was equipped with four 5-mm strain gages, which were attached at mid-height and evenly distributed around the circumference. Micro-Measurements CEA-00-125-UNA-350 strain gages were utilized because they are made for Invar metal.

Prior to adhering the strain gages, each area underwent a sanding process, starting with grit #40 and progressing up to grit #600, until a mirror-like surface was reached. Subsequently, the surface was cleaned using an acidic solution, followed by neutralization. The strain gages were then affixed with adhesive and covered with tape to protect them from any potential damage.

The measurement system was set up to record strain at 15-minute intervals, commencing approximately 10 minutes after the concrete pouring process.

Four thermocouples were positioned at the mid-height of the Invar rings, with two placed on the inner ring and two on the outer ring. All thermocouples were affixed to the side of the rings opposite the concrete specimen using tape to secure their position.

4.2.2 Temperature Control System

After four days, an external cooling system was used to induce cracking. The temperature control system consisted of an Anova A40 water bath system pumping ethylene glycol at 15 L/min through a looped copper coil (Figure 4.8). To distribute the temperature along the concrete ring, a 1/8” aluminum plate was placed on the top of the concrete, making contact with both the copper coil and the concrete.

Figure 4.8 Temperature control system. Source: Tanner Research Group

4.2.3 Insulating Chamber

The double-ring system was placed in an insulating chamber made of plywood and extruded polystyrene insulation, as shown in Figure 4.9, to maintain the temperature during cooling. To reduce the friction between the concrete and the plywood, a nonstick plastic sheet was attached between them. With this insulation system, the lower temperature limit of the equipment was achieved when the water bath reached a temperature of -30°C (-22°F) and the concrete inside the Invar rings was at -5°C (23°F).

Figure 4.9 Insulating chamber

4.2.4 Strain Gage Temperature Calibration

When using different temperature ranges, results using bonded strain gages can vary significantly due to the resistance change in the gage caused by temperature and being independent of mechanical strain. This source of error can be the most significant in this type of test (Micro-Measurements 2014). There are three basic methods of compensation available: the simultaneous recording of strain and temperature, temperature-compensating circuits, and self-temperature compensation (STC) (Hannah and Reed 1992).

Strain gage readings were corrected using an equation that takes into consideration the electrical resistivity of the gird conductor and the differential thermal expansion between the grid conductor and the material bonded to the strain gage. For this project, thermal output is given by Equation 4-1 when using Fahrenheit and Equation 4-2 for temperatures in Celsius degrees, as illustrated in Figure 4.10. Strains at a given temperature were subtracted from the measured strains.

$$\mu\varepsilon = -145 + 4.06T - 3.39x10^{-2}T^2 + 8.29x10^{-5}T^3 - 6.68x10^{-8}T^4$$ **Equation 4-1**

Where T is temperature in °F

$$\mu\varepsilon = -47 + 3.85T - 8.54x10^{-2}T^2 + 4.34x10^{-4}T^3 - 7.01x10^{-7}T^4$$ **Equation 4-2**

Where T is temperature in °C

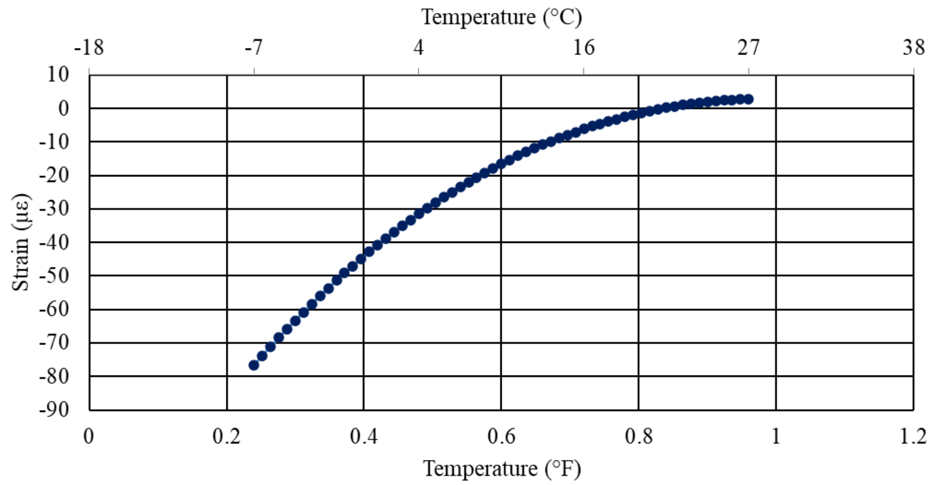

Figure 4.10 Thermal output of strain gages

4.2.5 Casting Procedures

The dual-ring specimens were placed in two lifts and rodded 75 times per lift to ensure good consolidation. The specimens were then finished by hand with a float and a trowel to achieve a relatively flat surface. For each batch of concrete, a minimum of nine 4 x 8-inch (100 x 200 mm) concrete cylinders were made to test mechanical properties.

5. RESULTS

5.1 Single-ring Testing

5.1.1 Mechanical Properties

Compressive and tensile strengths were tested for each batch following the corresponding Standard Test Method (ASTM C39 2021) (ASTM C496 2017). Compressive strength results of each mixture are reported in Table 5.1, and tensile strength results are reported in Table 5.2.

Table 5.1 Compressive strength results for single ring batches

Mixture	Compressive Strength, psi (MPa)	Coefficient of variation
GR-F0S0	2962 (20.42)	7.8%
GR-F8S0	2980 (20.55)	7.0%
GR-F0S2	2758 (19.01)	6.8%
GR-F8S2	2891 (19.93)	2.0%

Table 5.2 Tensile strength results for single ring batches

Mixture	Tensile Strength, psi (MPa)	Coefficient of variation
GR-F0S0	438 (3.02)	12.2%
GR-F8S0	391 (2.70)	4.4%
GR-F0S2	363 (2.50)	8.8%
GR-F8S2	352 (2.43)	6.0%

Mechanical properties of each mixture were analyzed to determine the relationship between the use of mitigation methods and their strengths. Compressive strength of the four batches is summarized in Figure 5.1. The use of fibers has no significant impact on the compressive strength of the control mix. Furthermore, the incorporation of SRA into the mix reduced the compressive strength by 7%. When combining SRA with fibers, this reduction was less noticeable, reducing it by merely 2.4%. The average tensile strength is 13% of the compressive strength for all four mixtures.

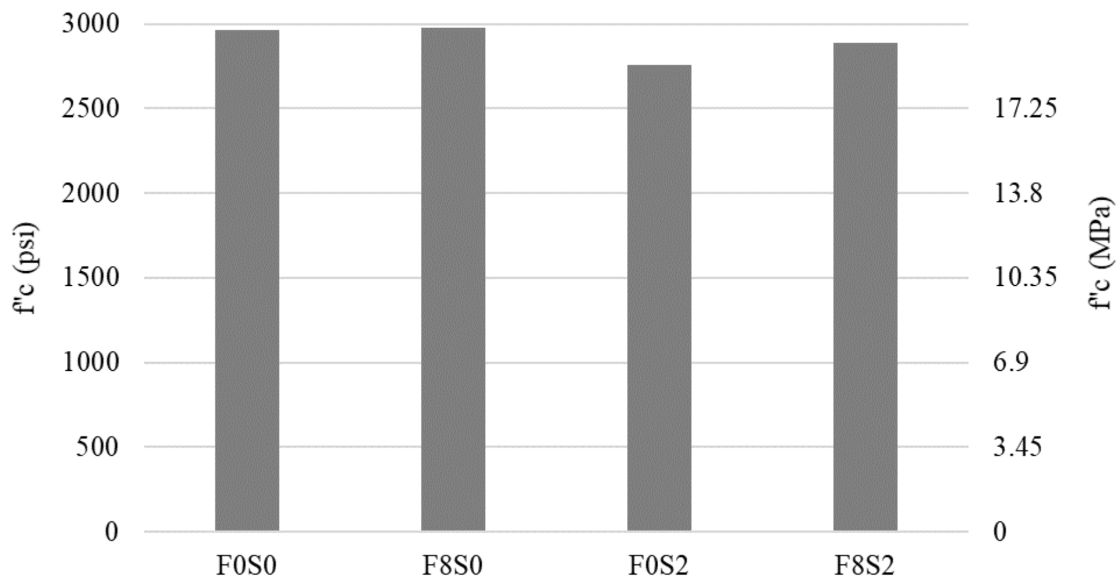

Figure 5.1 Compressive strength of single-ring mixtures

5.1.2 Age at Cracking

A first mixture designated as GR-F0S0 was evaluated using the single-ring test, and strains are illustrated in Figure 5.2. A sudden decrease in strain was noted at 25 hours, and that is defined as the cracking time. A second mix using 8% fibers, GR-F8S0, indicated cracking at 48 hours (Figure 5.3). The second mitigation method of SRA had a cracking time of 44.5 hours (Figure 5.4). A final specimen with both mitigation methods indicated that cracking occurred at 102 hours (Figure 5.5).

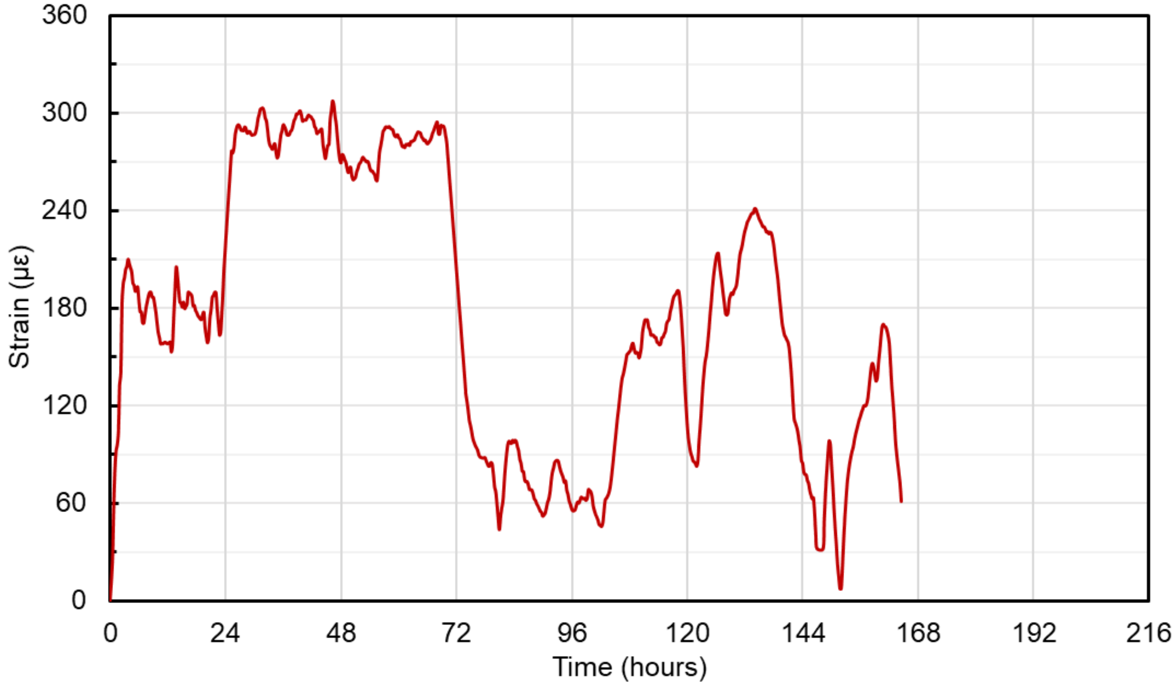

Figure 5.2 SR-GR-F0S0

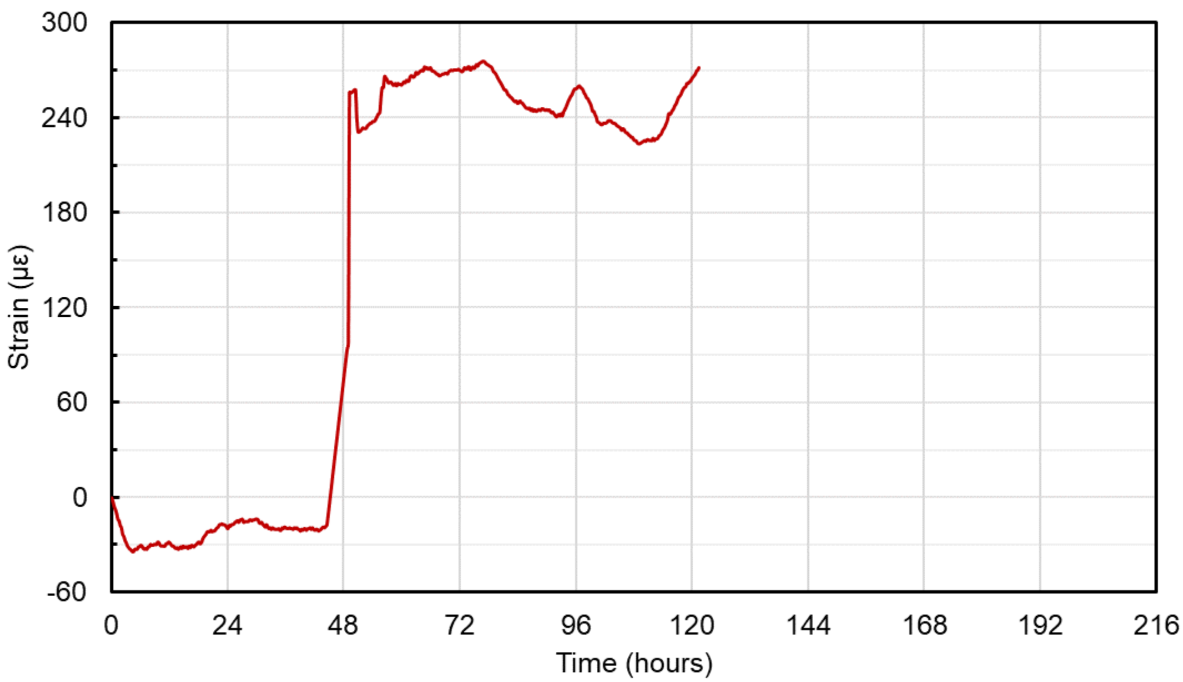

Figure 5.3 SR-GR-F8S0

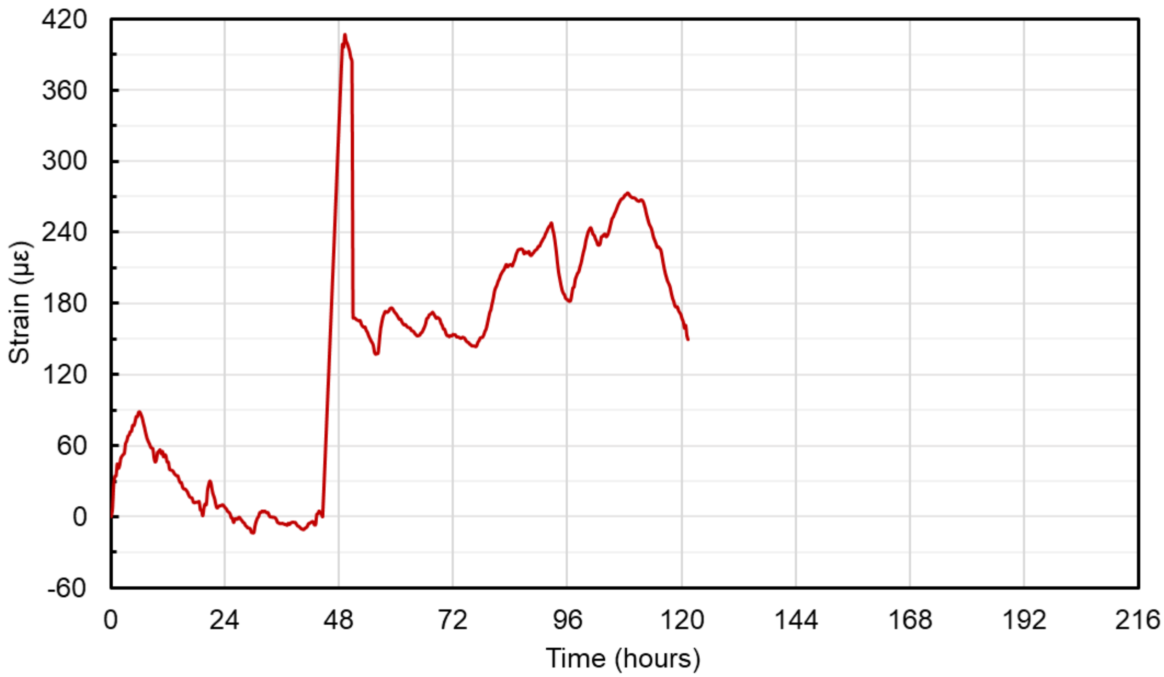

Figure 5.4 SR-GR-F0S2

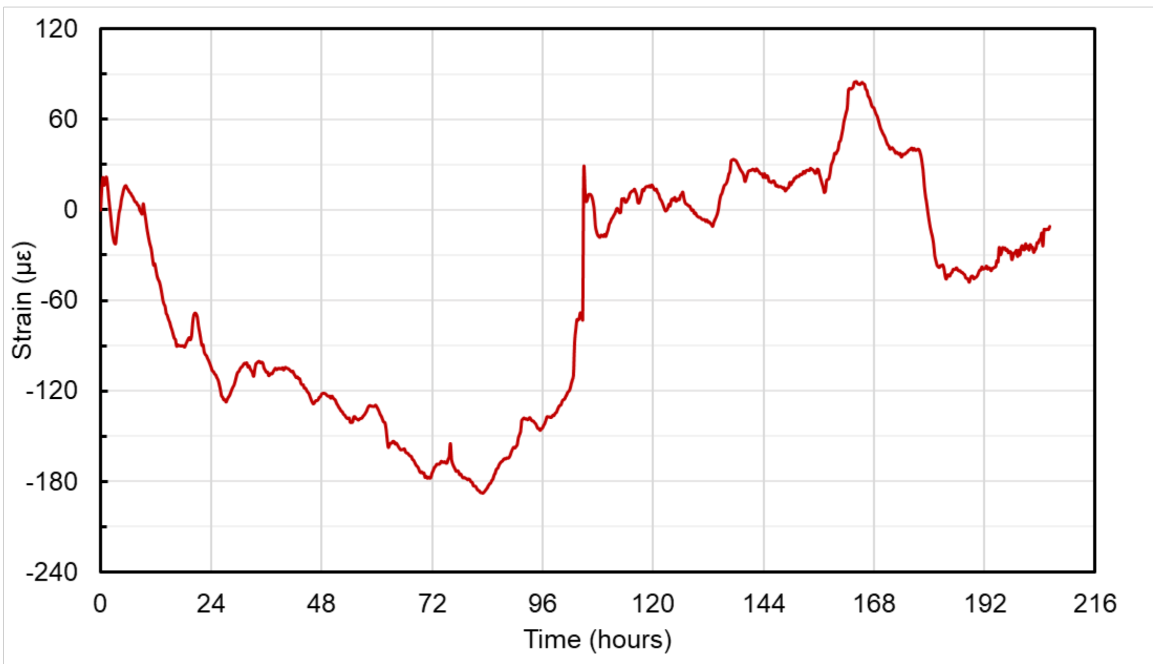

Figure 5.5 SR-GR-F8S2

Figure 5.6 compares time to cracking from all four specimens. All mitigation measures delayed cracking. The control mix cracked at 25 hours. Mitigating using fibers, SRA, and the combination of both measures resulted in cracking times of 48, 44, and 102 hours, respectively. When compared with the control specimens, the cracking times increased by factors of 1.92 (48/25), 1.78, and 4.08, respectively.

For this set of results, fibers performed slightly better than SRA, delaying the cracking time. The combination of fibers with SRA resulted in the largest cracking delay, indicating that combining mitigation measures is the ideal solution.

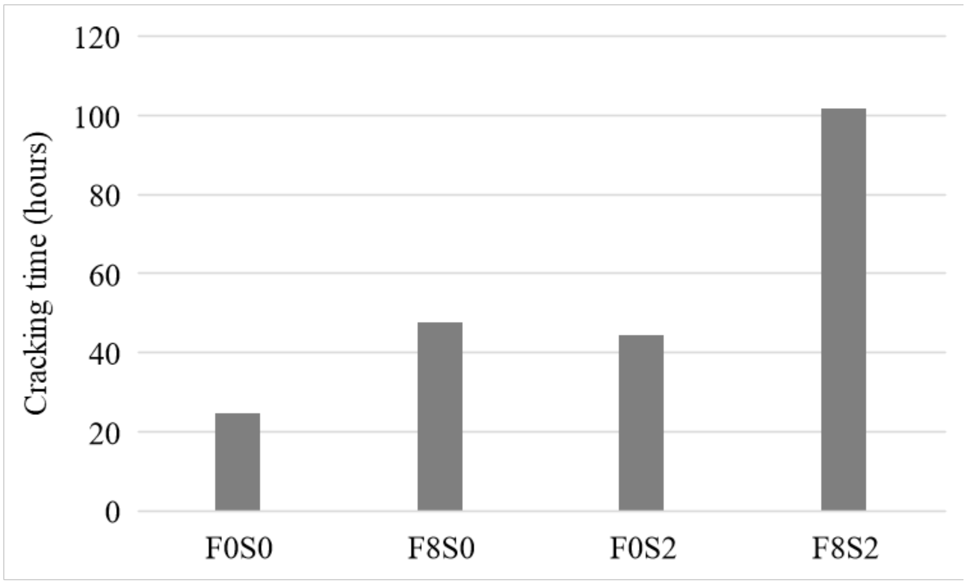

Figure 5.6 Summary of cracking time of single-ring mixtures

5.2 Dual-ring Testing

5.2.1 Mechanical Properties

Compressive strength was evaluated for every mixture used in the dual ring testing in accordance with ASTM C39 (ASTM C39 2021), and results are reported in Table 5.3.

Table 5.3 Compressive strength results for dual ring batches

Mixture	Compressive Strength, psi (MPa)	Coefficient of variation
GR-F0S0	3612 (24.90)	5%
GR-F8S0	3532 (24.35)	3%
GR-F0S2	2622 (18.08)	4%
GR-F8S2	3530 (24.34)	3%

A comparison of compressive strengths of the four mixtures is illustrated in Figure 5.7. The addition of fibers or fibers with SRA did not show any significant changes in the final compressive strength of the control mixture. On the other hand, the use of SRA in the mixture decreases the compressive strength by 27%. Some investigators report increases (Wang, Banthia and Zhang 2012) and (Wang, Chia, et al. 2013); and others report decreases (Maia, et al. 2012), (Güneyisi, Gesoglu, et al. 2014), (Yoo, et al. 2015), and

(Oliveira, Ribeiro and Branco 2014). This can be attributed to the delay that the admixture produces in the hardening process.

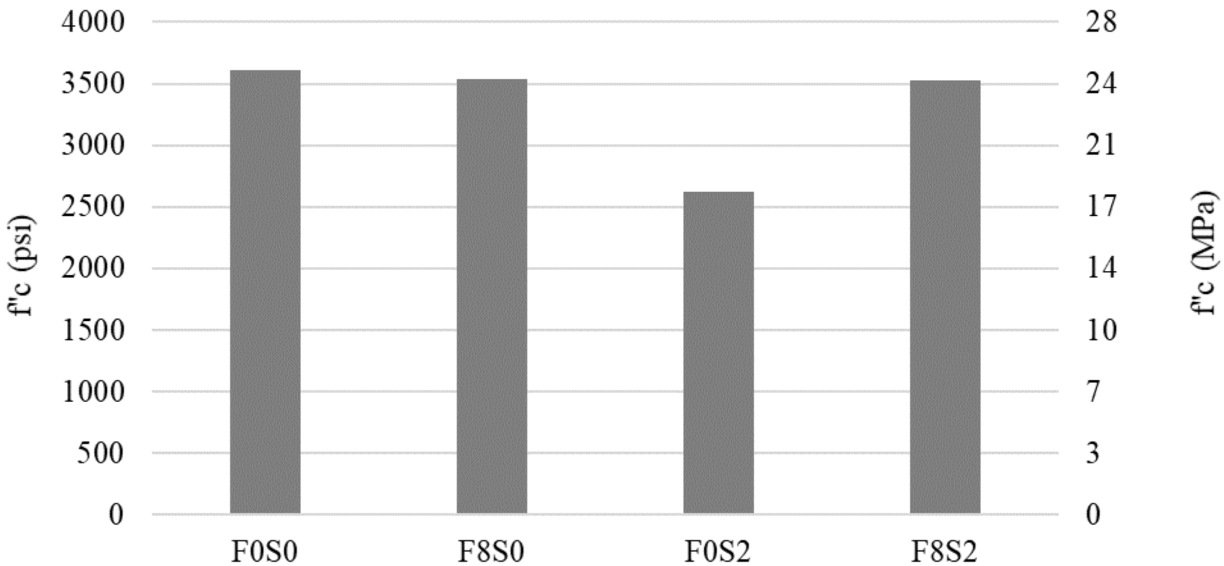

Figure 5.7 Compressive strength of dual-ring mixtures

5.2.2 Age at Cracking

A control specimen designated as DR-GR-F0S0 was evaluated using the dual-ring test, as illustrated in Figure 5.8. The first sudden decrease of a 20 micro strain or more occurred at 35 hours, defined as the cracking time (Figure 5.9). The second specimen used fibers, DR-GR-F8S0, and strain measurements are shown in Figure 5.10; a more detailed view in Figure 5.11 shows that cracking occurred at 117 hours. The second mitigation method used SRA, and strains illustrated in Figure 5.12 identify a cracking time of 108 hours, which is detailed in Figure 5.13. Strains measured from combined mitigation methods are illustrated in Figure 5.14. In this case, cracking was not observed during the length of the experiment (206 hours).

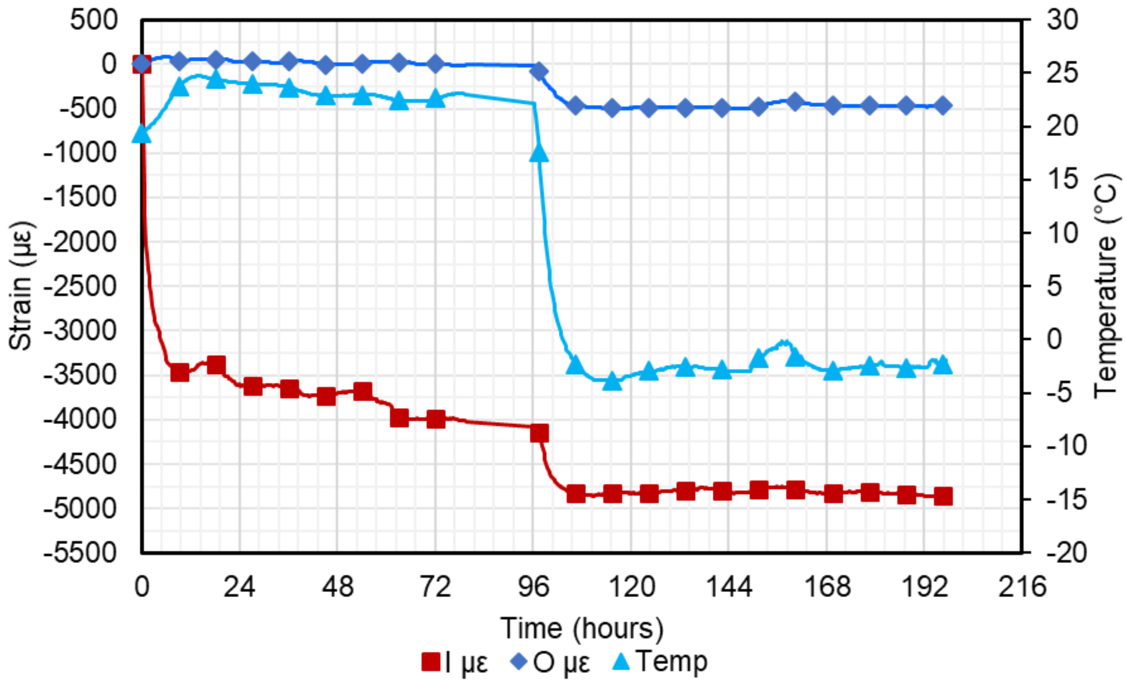

Figure 5.8 DR-GR-F0S0

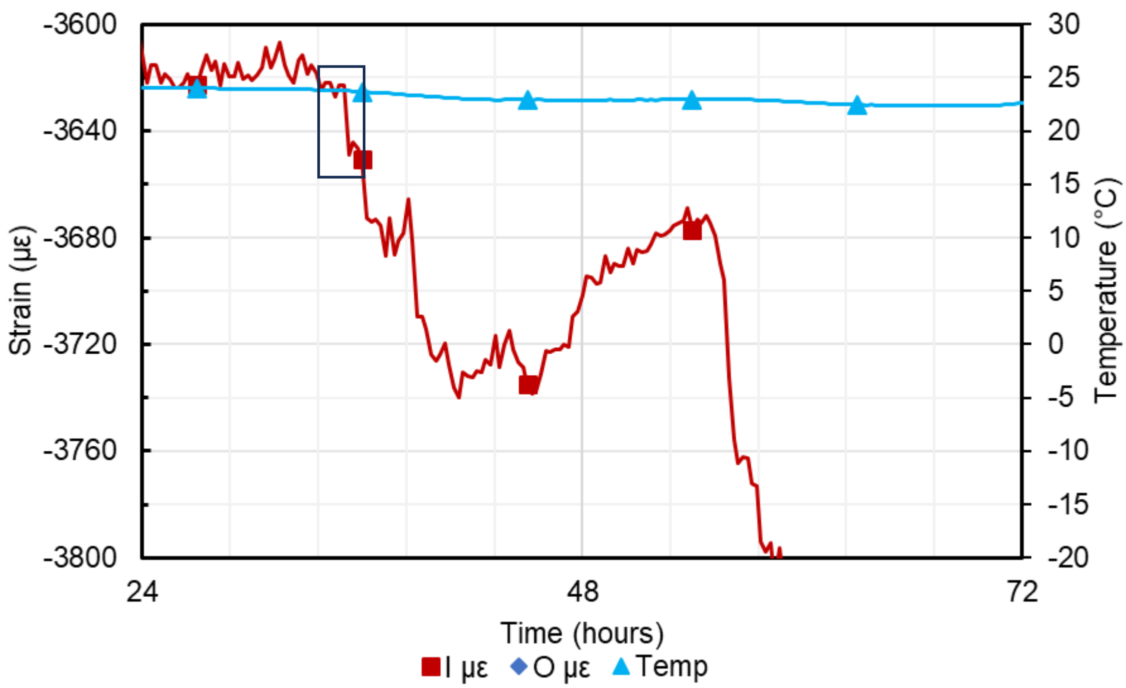

Figure 5.9 DR-GR-F0S0 cracking time

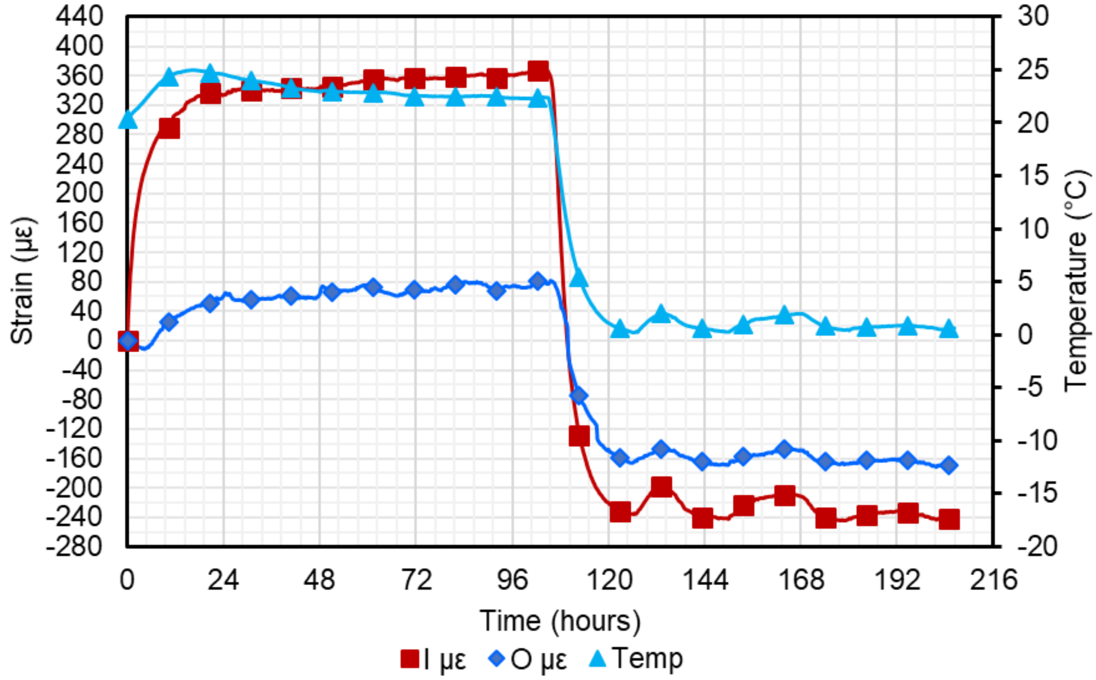

Figure 5.10 DR-GR-F8S0

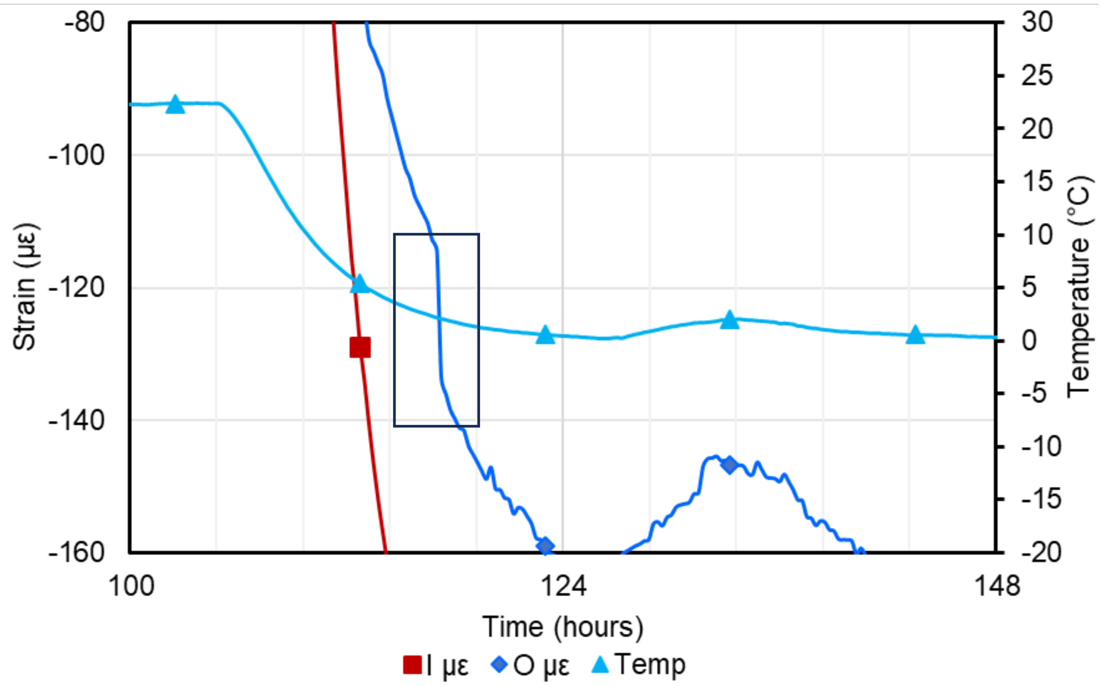

Figure 5.11 DR-GR-F8S0 cracking time

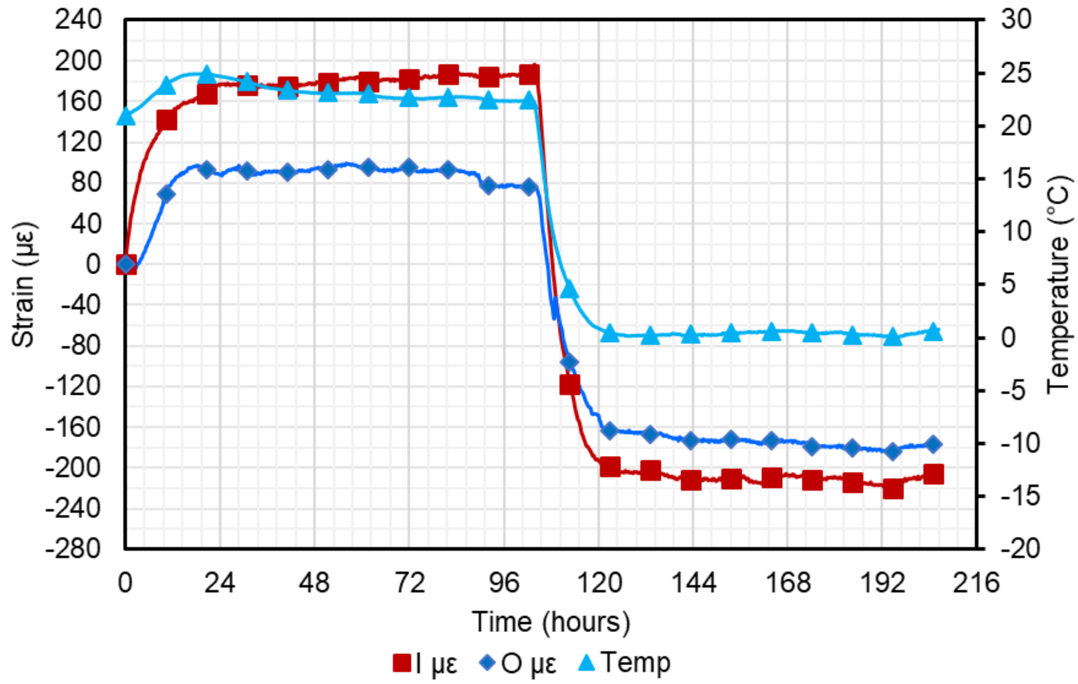

Figure 5.12 DR-GR-F0S2

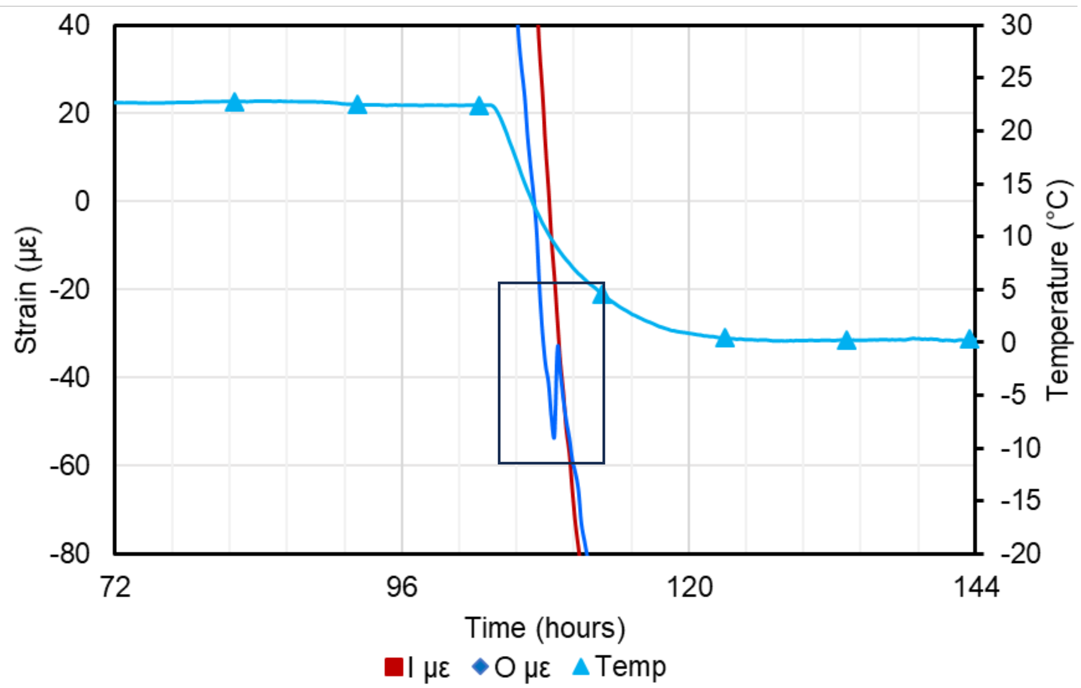

Figure 5.13 DR-GR-F8S0 cracking time

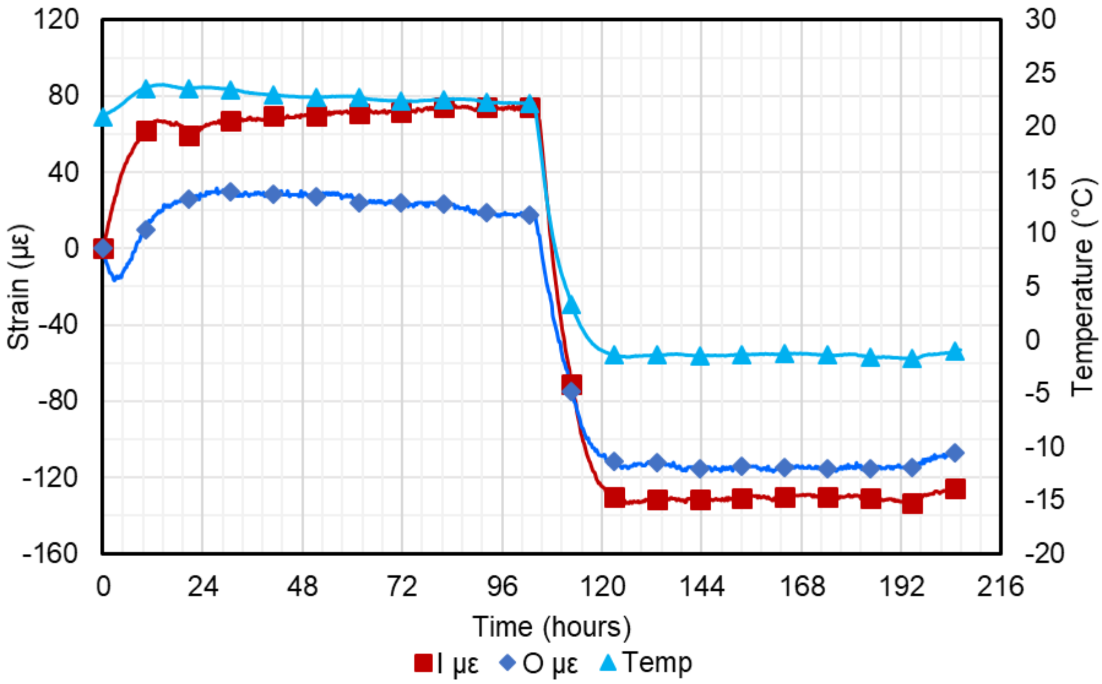

Figure 5.14 DR-GR-F8S2

Figure 5.15 illustrates time to cracking for dual-ring test results. The combination of fibers with SRA performed better than any other mitigation method by extending the cracking time by a factor of 5.88. Comparing the use of fibers to adding SRA to the control mixture, both improved cracking time, where fibers improved results by a factor of 3.34 and SRA by 3.08. These results are in agreement with previous studies where it was found that the addition of similar doses of fibers have a minimum reduction in shrinkage of 25% (Myers, Kang and Ramseyer 2008) and a 2% addition of SRA improves shrinkage by a factor of 1.4 (Maia, et al. 2012).

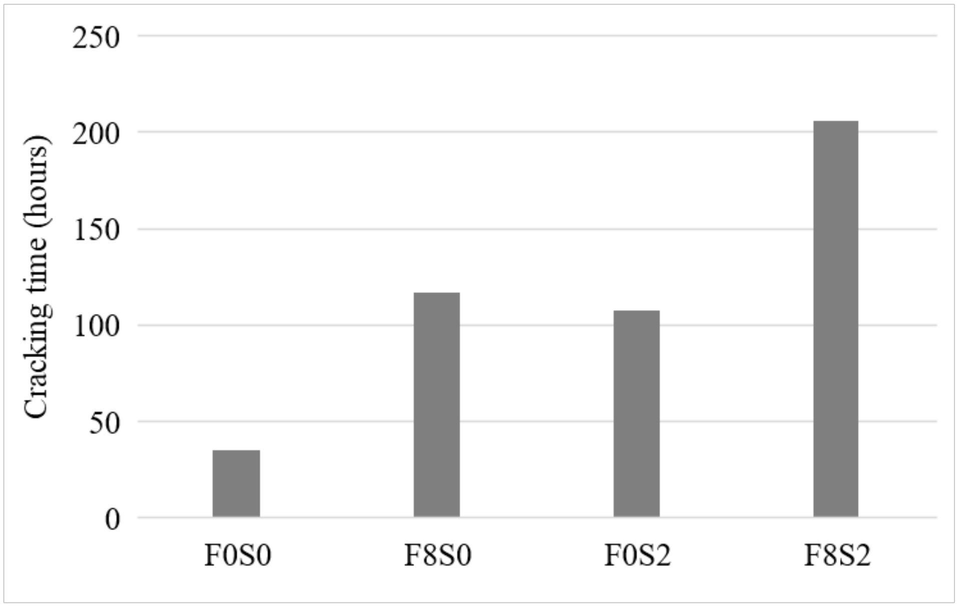

Figure 5.15 Summary of cracking time of dual-ring mixtures

5.3 Comparison of Results

Results for both the single-ring and dual-ring experiments are compared in Figure 5.16. In general, the results between the two types of experiments are consistent: the control mixture had the shortest time to cracking; the mixture with SRA cracked, followed very closely by the mix with fibers; and the combination of SRA with fibers had the most significant improvement in the cracking time.

It is important to mention that although both the single-ring and the dual-ring are designed with the same level of restraint, the single-ring specimens exhibited earlier cracking for all the experiments with an average of 50% of the cracking time of the dual-ring experiments.

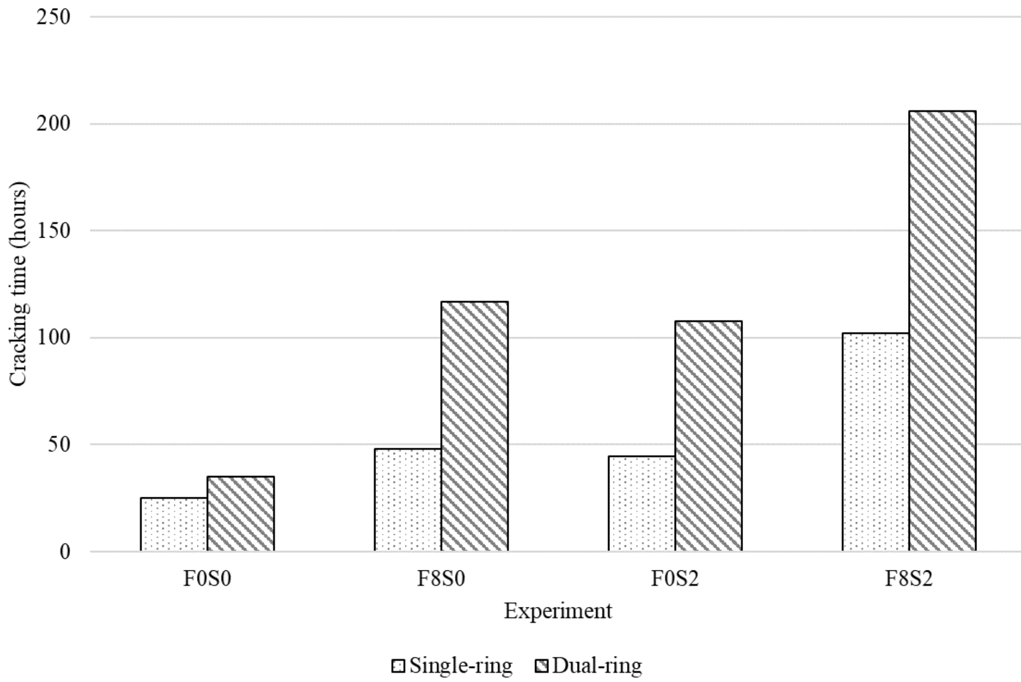

Figure 5.16 Comparison of cracking time of DR and SR

6. CONCLUSIONS

This experimental study evaluated the effectiveness of two different mitigation methods and the combination of these for granite mixtures: incorporation of 8 lb/yd^3 (4.75 kg/m^3) of polypropylene fibers, 2% of replacement by weight of cementitious materials, and the combination of both mitigation measures. The evaluation was performed using two different methods: single-ring and dual-ring. Mechanical properties such as compressive strength and tensile strength were studied for each mixture. According to the experiment results, the conclusions can be drawn as follows:

1. The incorporation of fibers into the mixture had limited impact on the mechanical properties, but roughly doubled the time to cracking.

2. The addition of SRA into the mix decreased compressive strength by an average of 17%, with a 90% improvement in cracking time.

3. When the combination of 8 lb/yd^3 (4.75 kg/m^3) of fibers with 2% of cementitious material replacement of SRA was used, the compressive strength of the improved mix was approximately the same. This method proved to be the most effective measure for delaying cracking time when using granite aggregate, by lengthening the cracking time by an average of five times the original cracking.

7. REFERENCES

AASHTO. *Standard Method of Test for Evaluating Stress Development and Cracking Potential due to Restrained Volume Change Using Dual Ring Test.* Washington, DC, 2017.

«AASHTO T334.» En *Standard Method of Test for Estimating the Cracking Tendency of Concrete*. Washington, DC, 2022.

Aghaee, Kamran, y Kamal H. Khayat. «Effect of shrinkage-mitigating materials on performance of fiber-reinforced concrete - An overview.» *Construction and Building Materials*, 2021.

Almusallam, A. A., M. Maslehuddin, M. Abdul-Waris, y M. M. Khan. «Effect of mix proportions on plastic shrinkage cracking of concrete in hot enviroments.» *Construction and Building Materials*, 1998: 353-358.

«ASTM C150 .» En *Standard Specification for Portland Cement*. West Conshohocken, PA, 2021.

«ASTM C1579.» En *Evaluating Plastic Shrinkage Cracking of Restrained Fiber Reinforced Concrete (using a Steel Form Insert)*. 2021.

«ASTM C305.» En *Standard Practice for Mechanical Mixing of Hydraulic Cement Pastes and Mortars of Plastic Consistency*. 2020.

«ASTM C39.» En *Standard Test Method for Compressive Strength of Cylindrical Concrete Specimens*. 2021.

«ASTM C496.» En *Standard Test Method for Splitting Tensile Strength of Cylindrical Concrete Specimens*. 2017.

ASTM International. «ASTM C1581.» En *Determining Age at Cracking and Induced Tensile Stress Characteristics of Mortar and Concrete under Restrained Shrinkage*. 2018.

Barret, T.J., I. De La Varga, y W.J. Weiss. «Reducing Cracking in Concrete Structures by Using Internal Curing with High Volumes of Fly Ash .» *Structures Congress* . ASCE, 2012.

Bolander, John E. *Controlling Temperature and Shrinkage Cracks in Bridge Decks and Slabs.* California Department of Transportation, 2018.

Boshoff, William P., y Riaan Combrinck. «Modelling the severity of plastic shrinkage cracking in concrete.» *Cement and Concrete Research*, 2013: 34-39.

Chilwesa, M., A. Akbarnezhad, M. Gharehchaei, A. Castel, R. Lloyd, y S. Foster. «Using the Double Ring Test to Assess the Effect of Type of Aggregate Used on Thermal Cracking Potential of Concrete.» *Proceedings of the 25th Australasian Conference on Mechanics of Structures and Materials.* Springer, 2020. 337-347.

De la Varga, Igor, Robert Spragg, Jose Muñoz, Michelle Helsel, y Benjamin Graybeal. «Cracking, Bond, and Durability Performance of Internally Cured Cementitious Grouts for Prefabricated Bridge Element Connections.» *Sustainability*, 2018.

De la Varga, Igor, Robert Spragg, Rafic El-Helou, y Benjamin Graybeal. «Shrinkage Cracking Propensity of UHPC.» *International Interactive Symposium on Ultra-High Performance Concrete.* Iowa State University Digital Press, 2019.

Elzokra, Ahmed, Ausamah Al Houri, Ahed Habib, Maan Habib, y Ahmad B. Malkawi. «Shrinkage Behavior of Conventional and Nonconventional Concrete: A Review.» *Civil Engineering Journal*, 2020: 1839-1851.

Gilbert, Ian R., A. Castel, I Khan, W. South, y J. Mohammadi. «An Experimental Study of Autogenous and Drying Shrinkage.» *High Tech Concrete: Where Technology and Engineering Meet*, 2018.

Gribniak, Viktor, Gintaris Kaklauskas, y Darius Bacinskas. «State-of-art review of shrinkage effect on cracking and deformations of concrete bridge elements.» *The Baltic Journal of Road and Brige Engineering*, 2007: 183-193.

Güneyisi, Erhan , Mehmet Gesoglu, Alaa Mohamadameen, Radhwan Alzeebaree, Zeynep Algın, y Kasım Mermerdas . «Enhancement of shrinkage behavior of lightweight aggregate concretes by shrinkage reducing admixture and fiber reinforcement.» *Construction and Building Materials*, 2014: 91-98.

Güneyisi, Erhan, Mehmet Gesoğlu, Alaa Mohamadameen, Radhwan Alzeebaree, Zeynep Algın, y Kasim Mermerdaş. «Enhancement of shrinkage behavior of lightweight aggregate concretes by shrinkage reducing admixture and fiber reinforcement.» *Construction and Building Materials*, 2014: 91-98.

Han, Yudong, Jun Zhang, Yiming Luosun, y Tingyu Hao. «Effect of internal curing on internal relative humidity and shrinkage of high strength concrete slabs.» *Construction and Building Materials*, 2014: 41-49.

Hannah, R. L., y S. Reed. *Strain Gage Users' handbook.* Elsevier Applied Science, 1992.

Hasan, Nausherwan. *Durability and Sustainability of Concrete.* New York: Springer Cham, 2020.

Holt, Erika. «Contribution of mixture design to chemical and autogenous shrinkage of concrete at early ages.» *Cement and Concrete Research*, 2005: 464-472.

—. *Early age autogenous shrinkage of concrete.* University of Washington, 2001.

Houst, Yves. «Carbonation shrinkage of hydrated cement paste.» *4th CANMET/ACI International Conference on Durability of Concrete.* Ottawa, Canada, 1997. 481-491.

«Influence of shrinkage reducing admixtures on distinct SCC mix compositions.» s.f.

Karagüler, Mustafa Erkan, y Mehmet Serkan Yatağan. «Effect of aggregate size on the restrained shrinkage of the concrete and mortar.» *MOJ Civil Engineering*, 2018.

Kosmatka, Steven H. , y Michelle L. Wilson. *Design and Control of Concrete Mixtures.* Portland Cement Association, 2011.

Li, Hua, Qian Tian, Haitao Zhao, Anqun Lu, y Jiaping Liu. «Temperature sensitivity of mgo expansive agent and its application in temperature crack mitigation in shiplock mass concrete.» *Construction and Building Materials*, 2018: 613-618.

Linmei, Wu, Nima Farzadnia, Caijun Shi, Zuhua Zhang, y Hao Wang. «Autogenous shrinkage of high performance concrete: A review.» *Construction and Building Materials*, 2017: 62-75.

Liu, Jianhui, Caijun Shi, Xianwei Ma, Kamal H. Khayat, Jian Zhang, y Dehui Wang. «An overview on the effect of internal curing on shrinkage of high performance cement-based materials.» *Construction and Building Materials*, 2017: 702-712.

Lofgren, I., y O. Esping. «Early Age Cracking of Self-Compacting Concrete.» *International RILEM Conference on Volume Changes of Hardening Concrete: Testing and Mitigation.* Lyngby: Technical University of Denmark, 2006.

Lura, Pietro, Brad Pease, Guy B. Mazzotta, Farshad Rajabipour, y Jason Weiss. «Influence of Shrinkage-Reducing Admixtures on Development of Plastic Shrinkage Cracks.» *ACI Materials Journal*, 2007: 187-194.

Maia, Lino, Helena Figueiras, Sandra Nunes, Miguel Azenha, y Joaquim Figueiras. «Influence of shrinkage reducing admixtures on distinct SCC mix compositions.» *Construction and Building Materials*, 2012: 304-312.

Matalkah, Faris, Talal Salem, Mamoon Shaafaey, y Parviz Soroushian. «Drying shrinkage of alkali activated binders cured at room temperature.» *Construction and Building Materials*, 2019: 563-570.

Mehta, P. Kumar, y Paulo J. M. Monteiro. *Concrete: Microstructure, Properties, and Materials.* New York: McGraw-Hill Education, 2014.

Meininger, R.C. *Drying Shrinkage of Concrete.* Silver Spring: National Ready Mixed Concrete Association, 1966.

Micro-Measurements. «TN-504-1.» *Strain Gage Thermal Output and Gage Factor Variation with Temperature*, 2014.

Myers, Daniel, Thomas H.K. Kang, y Chris Ramseyer. «Early-Age Properties of Polymer Fiber-Reinforced Concrete.» *International Journal of Concrete Structures and Materials*, 2008: 9-14.

Oliveira, Miguel, Antonio Ribeiro, y Fernando Branco. «Combined effect of expansive and shrinkage reducing admixtures to control autogenous shrinkage in self-compacting concrete.» *Construction and Building Materials*, 2014: 267-275.

Pease, Bradley, William Jason Weiss , y Hardik Shah. «Restrained shrinkage behavior of mixtures containing shrinkage reducing admixtures and fibers.» 2005.

Pillar, N. M. P., y W.L. Repette. «The effect of fibers on the loss of water by evaporation and shrinkage of concrete.» *Ibracon Structures and Materials Journal*, 2015: 8-13.

Powers, T.C. «Causes and Control of Volume Change.» *Journal PCA Research Laboratories*, 1959: 29-39.

Qi, C., J. Weiss, y J. Olek. «Characterization of plastic shrinkage cracking in fiber reinforced concrete using image analysis and a modified Weibull function.» *Materials and Structures*, 2003: 386-395.

Raoufi, Kambiz, John Schlitter, Dale Bentz, y Jason Weiss. «Parametric Assessment of Stress Development and Cracking in Internally Cured Restrained Mortars Experiencing Autogenous Deformations and Thermal Loading.» *Advances in Civil Engineering*, 2011: 1-16.

Sakata, Kenji , y Takumi Shimomura. «Recent Progress in Research on and Code Evaluation of Concrete Creep and Shrinkage in Japan .» *Journal of Advanced Concrete Technology* , 2004: 133-140.

Saladi, Naveen, Robert Spragg, y Igor De la Varga. «Effects of Internal Curing on Inclusion in Prepackaged Cementitious Grout and Ultra-High Performance Concrete Materials.» *Sustainability*, 2022.

Schlitter, John, Ryan Henkensiefken, Javier Castro, Kambiz Raoufi, y Jason Weiss. *Development of Internally Cured Concrete for Increased Service Life.* Joint Transportation Research Program, 2010.

Shh, S.P., M. E. Krguller, y M. Sarigaphuti. «Effects of Shrinkage-Reducing Admixtures on Restrained Shrinkage Cracking of Concrete.» *Materials Journal*, 1992: 289-295.

Sofi, Massoud, Daksh Baweja, Priyan Mendis, y Ellya Elvira. «Anchorage zones behaviour of early age concrete: Application to post-tensioned members.» *Construction and Building Materials*, 2014: 1-12.

Tang, Shengwen, Desheng Huang, y Zhen He. «A review of autogenous shrinkage models of concrete .» *Journal of Building Engineering*, 2021.

Tazawa, Ei-ichi, y Shingo Miyazawa. «Experimental Study on Mechanism of Autogenous Shrinkage of Concrete.» *Cement and Concrete Research*, 1995: 1633-1638.

Tremper, B., y D.L. Spellman. *Shrinkage of Concrete-Comparison of Laboratory and Field Performance.* Washington D.C.: Highway Research Record No. 3, 1963.

Van breugel, K. «Prediction of Temperature Development in Hardening Concrete.» *Rilem Report 15*, 1998: 51-57.

Wang, Jun-Yan, Kok-Seng Chia, Jat-Yuen Richard Liew, y Min-Hong Zhang. «Flexural performance of fiber-reinforced ultra lightweight cement.» *Cement & Concrete Composites*, 2013: 39-47.

Wang, Jun-Yan, Nemkumar Banthia, y Min-Hong Zhang. «Effect of shrinkage reducing admixture on flexural behaviors of fiber.» *Cement & Concrete Composites*, 2012: 443-450.

Wang, Yuli, Hang He, Junjie Wang, Fanghui Li, Yahong Ding, y Lei Xu. «Effect of aggregate micro fines in machine-made sand on bleeding, autogenous shrinkage and plastic shrinkage cracking of concrete.» *Materials and Structures*, 2022: 106.

Wasala, W.M.T.D., y H.D. Yapa. «Prediction of Temperature Development in Concrete using Semi-adiabatic Temperature Measurements.» *Engineer Journal of the Institution of Engineers Sri Lanka*, 2017: 1-8.

Weiss, Jason. *Guidance to Reduce Shrinkage and Restrained Shrinkage Cracking.* National Concrete Pavement Technology Center, 2022.

White, George R. *Basic Concrete Construction Practices.* Portland Cement Association, 1975.

Wilson, Cameron, y Jason Weiss. «Improving the Durability of High Early Strength (HES) Concrete Patching Materials for Concrete Pavements.» *Transportation Research Records*, 2020: 12-23.

Xi, Yunping, y otros. *Assesment of the cracking problem in newly constructed bridge decks in Colorado.* Colorado Department of Transportation Research Branch, 2003.

Xia, Qiang, Hua Li, Ting Yao, Anqun Lu, Qian Tian, y Jiaping Liu. «Cracking behaviour of restrained cementitious materials with expansive agent by comprehensive analysis of residual stress and acoustic emission signals.» *Advances in Cement Research*, 2017: 81-90.

Xu, Yunsheng, y D.D.L. Chung. «Reducing the drying shrinkage of cement paste by admixture surface treatments.» *Cement and Concrete Research* , 2000: 241-245.

Yoo, Doo-Yeol, Jihwan Kim, Goangseup Zi, y Young-Soo Yoon. «Effect of shrinkage-reducing admixture on biaxial flexural behavior of ultra-high-performance fiber-reinforced concrete.» *Construction and Building Materials*, 2015: 67-75.

Zhan, Pei-min, y Zhi-hai He. «Application of Shrinkage Reducing Admixture in Concrete: A Review.» *Construction and Building Materials*, 2019: 676-690.

8. APPENDIX A. Average Temperatures of Wyoming